

Interference Mitigation via Rate-Splitting and Common Message Decoding in Cloud Radio Access Networks

Alaa Alameer Ahmad^{*}, *Student Member, IEEE*, Hayssam Dahrouj[†], *Senior Member, IEEE*, Anas Chaaban[‡], *Senior Member, IEEE*,

Aydin Sezgin^{*}, *Senior Member, IEEE* and Mohamed-Slim Alouini[§], *Fellow, IEEE*

Abstract

Cloud-radio access networks (C-RAN) help overcoming the scarcity of radio resources by enabling dense deployment of base-stations (BSs), and connecting them to a central-processor (CP). This paper considers the downlink of a C-RAN, where the cloud is connected to the BSs via limited-capacity backhaul links. The paper proposes splitting the message of each user into two parts, a private part decodable at the intended user only, and a common part which can be decoded at a subset of users, as a means to enable large-scale interference management in CRAN. To this end, the paper optimizes a transmission scheme that combines rate splitting (RS), common message decoding (CMD), clustering and coordinated beamforming. The paper focuses on maximizing the weighted sum-rate subject to per-BS backhaul capacity and transmit power constraints, so as to jointly determine the RS-CMD mode of transmission, the cluster of BSs serving private and common messages of each user, and the associated beamforming vectors of each user private and common messages. The paper proposes solving such a complicated non-convex optimization problem using l_0 -norm relaxation techniques, followed by inner-convex approximations (ICA), so as to achieve stationary solutions to the relaxed non-convex problem. Numerical results show that the proposed method provides significant performance gain as compared to conventional interference mitigation techniques in CRAN which treat interference as noise (TIN).

Part of this paper was presented at the IEEE International Workshop on Signal Processing Advances in Wireless Communications (SPAWC), Kalamata, Greece, June 2018 [1].

A. A. Ahmed and A. Sezgin are with the Department of Electrical Engineering Ruhr-university Bochum, Germany (Email: {alaa.alameerahmad, aydin.sezgin}@rub.de). H. Dahrouj is with the Department of Electrical and Computer Engineering, Effat University, Saudi Arabia (Email: hayssam.dahrouj@kaust.edu.sa). A. Chaaban is with the School of Engineering, The University of British Columbia, Kelowna, Canada (Email: anas.chaaban@ubc.ca). M. S. Alouini is with the Communication Theory Lab, King Abdullah University of Science and Technology, Thuwal, Saudi Arabia (Email: slim.alouini@kaust.edu.sa).

I. INTRODUCTION

A. Overview

Motivated by the scarcity of radio resources and the ever increasing need for higher data rates and reliable wireless services, C-RAN provides a practical network architecture capable of boosting the spectral and energy efficiency in next generation wireless systems (5G and beyond) [2]–[4]. By connecting many BSs to the CP, C-RANs enable spatial reuse through dense deployment of small cells, and exploit the emerging cloud-computing technologies for managing large networks [5], [6].

With ultra dense deployment of small cells, the distance between the base station (BS) and the end user decreases, which results in a better quality of the direct channel. This comes, however, at the cost of increasing inter-BS interference due to proximity of the BSs in neighbouring cells. Furthermore, in C-RAN, the performance of the system is also limited by the finite capacity of backhaul links, [7]–[13]. Intuitively, in the extreme case when the backhaul capacity goes to infinity, the C-RAN is equivalent to a broadcast channel (BC). In the other extreme in which the backhaul links have zero-capacity, the C-RAN becomes equivalent to an interference channel (IC), the capacity of which is still a well-known open problem, even for the simple two-user IC, where treating interference as noise (TIN) is known to be a suboptimal strategy, especially in high-interference regimes [14], [15]. With limited backhaul capacity, C-RAN bridges the two extremes. With this observation in mind, we investigate in this paper a transmission scheme which improves the performance of C-RAN in different regimes, i.e., in backhaul limited regimes and interference limited regimes.

In the seminal works on IC [14], [15], it is shown that splitting the message of each user into two parts, a private part decodable at the intended user only and a common part which can be decoded by another user, can significantly approach the capacity region of the IC. Motivated by this fact, this paper studies rate-splitting in the realm of a CRAN. It proposes splitting the message of each user into two parts, a private part decodable at the intended user only, and a common part which can be decoded at a subset of users.

Since the CP is connected to the BSs in cloud-enabled networks, C-RAN becomes a particularly suitable platform for the physical implementation of rate-splitting strategies. In the context of our paper, all rate splitting and common message decoding (RS-CMD) techniques are adopted for the sole purpose of reducing large-scale interference. As the CP is connected to the BSs via

finite capacity backhaul links, it becomes equally important to determine the set of BSs (i.e., cluster) which serves each user, jointly with selecting the mode of transmission of each user (i.e., private, common, or both).

This work considers the RS-CMD problem in the downlink of a CRAN, where the CP is connected to several BSs, each equipped with multiple antennas. The CP applies central encoding to user's messages and establishes cooperation between a cluster of BSs by joint design of linear precoding in a user-centric clustering fashion, also known as *data-sharing* strategy [16]–[19], as it achieves a better performance compared to classical transmission schemes [20]. The paper then considers the problem of maximizing the weighted sum-rate (WSR) across the network, subject to per-BS backhaul capacity and transmission power constraints. The goal of this optimization is to jointly determine the RS-CMD mode of transmission, the cluster of BSs serving private and common messages of each user, and the associated beamforming vectors of each user private and common information. The paper provides an in-depth numerical investigation of the impact of RS-CMD strategy on the achievable rate in CRANs, and compares it with the conventional strategies which treat interference as noise.

B. Related Work

The contributions of this paper are related to works on rate splitting and common message decoding, clustering, and beamforming; topics which are studied in the literature of wireless systems, both individually and separately.

In rate-splitting schemes, the data of each user is divided into two parts: a private message which is decoded only at the interested user, and a common message which is decodable at interfering users. Reference [14] shows that such a RS-CMD technique leads to the largest known achievable rate-region in a 2-user IC. Such splitting strategy is further shown in [15] to achieve within one-bit from the capacity of the 2-user IC. Although being based on simple networks, those information-theoretical studies show the benefits of using RS-CMD techniques in high interference regimes. For instance, inspired by the theoretical works in [14], [15], the authors in [21] generalize this RS-CMD scheme to a practical multi-cell network showing significant achievable rate improvement by jointly designing the beamforming vectors for private and common information in RS-CMD as compared to beamforming design using TIN. In [22], the authors apply RS ideas to a practical setup of heterogeneous wireless networks. The results in [22] suggest that a significant performance gain can be reached by applying RS as compared

to rank-1 coordinated beamforming schemes that adopt TIN strategy. The work in [23] uses common message decoding and successive interference cancellation techniques to maximize the sum rate in multi-cell multi-user MIMO system. The difference of convex optimization technique is used to efficiently solve the difficult underlying optimization problem. Recently, RS-CMD has gained a noteworthy attention in the literature of medium access schemes. For instance, the authors in [24] propose a novel RS multiple access (RSMA) scheme, which generalizes and outperforms conventional multiple access schemes such as Space-Division Multiple Access (SDMA) and Non-Orthogonal Multiple Access (NOMA). Based on these results, the authors in [25] show that RSMA is more energy efficient than SDMA and NOMA. Reference [26], on the other hand, shows that linearly precoded RS is more efficient than the conventional Multi-User Linear Precoding (MU-LP) in terms of spectral and energy efficiency. Through numerical simulations, the authors in [26] particularly show that, with no increase in receiver complexity, RS achieves better performance metrics as compared to both NOMA and MU-LP systems. The above works, i.e., [14], [15], [21]–[26], however, do not address cloud-enabled scenarios, as they ignore the physical-layer considerations induced by RS-CMS in CRANs, and do not account for determining the set of common messages. This paper, therefore, focuses on the study of the joint resource allocation problem in CRAN, together with evaluating the impact of RS-CMD techniques. The paper further develops a well-chosen heuristic procedure to determine the set of common messages of each user.

In general, most of the existing works (e.g., [27]–[32]) on multi-cell interference mitigation in practical networks focus on doing so through jointly allocating resources (e.g., beamforming vectors and transmit power) in order to maximize a network utility. References [27]–[32], however, often adopt the strategy of TIN and assume an infinite backhaul capacity. Towards this end, the impact of finite backhaul links capacity is studied in the downlink of CRAN in [19]. The problem studied in [19] turns out to be a mixed-integer non linear problem (MINLP), which is solved by relaxing the discrete non-convex per-BS backhaul constraints using re-weighted l_1 -norm, and then by applying a generalized weighted minimum mean square algorithm (WMMSE). The authors in [7] consider the joint design of BSs' clusters and beamforming vectors to minimize the network-wide transmit power cost. The trade-off between the backhaul traffic and transmit power is also investigated in references [9]–[13], [19], all of which adopt TIN strategy to decode the received messages. At this point, it becomes essential to investigate how adopting RS-CMD can influence the design of clusters of BSs and the beamforming vectors associated with the

private and common messages in a CRAN setup. Towards this end, our current paper investigates the downlink C-RAN by utilizing a RS-CMD strategy, and focuses on evaluating its impact on jointly optimizing the beamforming vectors, the clustering and the transmission mode, so as to maximize the weighted-sum rate (WSR) across the network. To the best of authors' knowledge, this is the first work on CRAN which both studies the application of RS-CMD coupled with joint clustering and beamforming, and numerically illustrates the potential gain provided by RS-CMD over TIN.

C. Contributions

In this paper, we propose using RS-CMD in downlink C-RAN to jointly design user centric clusters of BSs, so as to explore RS-CMD benefits in large-scale interference management. We formulate a WSR maximization problem subject to per-BS backhaul capacity and per-BS transmit power constraints, so as to determine the RS splitting mode, the cluster of BSs which serves each user, and the beamforming vectors associated with the private and common messages parts. Such a problem is generally NP-hard due to its mixed discrete and continuous optimization nature, in addition to the non-convexity of the constraints. Our paper proposes solving such a problem using a heuristic based on l_0 -norm approximation to tackle the discrete part, followed by a polynomial time algorithm based on inner convex approximations, so as to find a stationary solution to the resulting non-convex continuous problem. The paper subsequently shows the numerical benefits of the proposed RS-CMD scheme in improving the achievable rates in C-RAN compared to the state-of-the art TIN strategy, both in the backhaul-limited and in the interference-limited regimes. Our main contributions can be summarized as follows:

- *Common Message Decoding (CMD) Set*: We propose a heuristic procedure for ordering the set of strongest interferers for each user, which consequently allows for determining the set of common messages to be decoded.
- *Clustering*: Based on l_0 -norm relaxation and inner-convex approximation framework, we propose a dynamic clustering approach. In the context of RS-CMD, we determine the set of BSs serving the private message and the set of BSs which serves the common message for each scheduled user. As opposed to the static clustering scheme described in [19], dynamic clustering procedure forms the clusters by taking into account the CMD set of each user, which can significantly affects the network connectivity. To deal with the non-convex backhaul constraint, the paper particularly proposes a surrogate convex function to

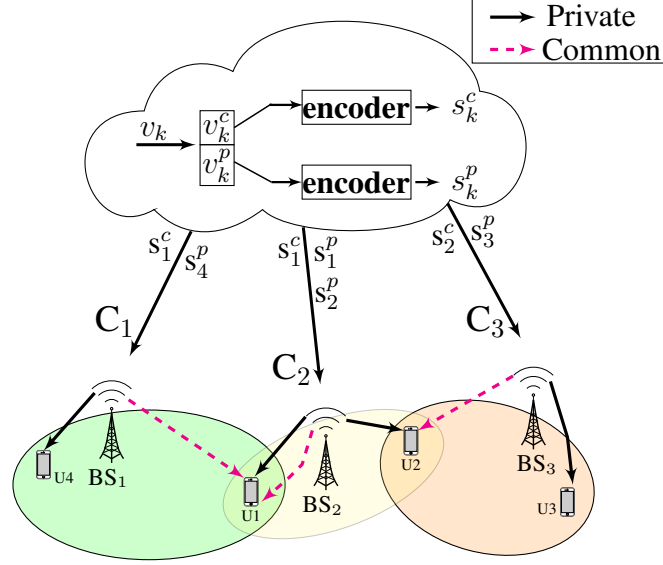


Figure 1: A C-RAN system with three cells. Both private and common messages are designed at the cloud.

approximate the backhaul constraint. The paper then compensates for such approximations using proper outer-loop updates in an iterative manner.

- *Beamforming*: Even when the clusters are fixed, the WSR problem with RS-CMD is not convex. This is because the private and common rate functions are non-convex in the private and common beamforming vectors, respectively. The paper, therefore, proposes solving such issue using an algorithm that applies well-chosen inner-convex approximations. The proposed algorithm is proven to converge in polynomial time to a stationary solution.
- *Numerical Simulations*: we show through extensive numerical simulations that our proposed solution outperforms the classical TIN in C-RAN. In both the interference limited and the backhaul limited regimes, we illustrate that RS-CMD makes a better use of the network resources in order to achieve higher rates as compared with TIN for different network parameters.

The rest of the paper is organized as follows. Section II illustrates the system model. Section III introduces the transmission scheme adopted in this work and formulates the WSR problem accordingly. The proposed solution is introduced in section IV. Section V presents the numerical simulations, and section VI concludes the paper.

II. SYSTEM MODEL

We consider a C-RAN system operating in downlink mode with a transmission bandwidth B . The network consists of a set of multi-antenna BSs $\mathcal{N} = \{1, 2, \dots, N\}$, serving a set of single-antenna users $\mathcal{K} = \{1, 2, \dots, K\}$. Each BS is equipped with $L \geq 1$ antennas. BS $n \in \mathcal{N}$ is connected to a CP, located at the cloud, via a backhaul link of capacity C_n . User k requires a message v_k , where the achievable data-rate at user k is denoted by R_k . All messages are jointly encoded at the CP into signals s_k , $\forall k \in \mathcal{K}$. The CP then shares combinations of s_k (or parts thereof) with the BSs through the backhaul links. This data-sharing is possible if the rate of signals shared with BS n does not exceed the backhaul capacity C_n . This is made more explicit when we describe RS in the next section. Upon receiving these signals, BS n constructs $\mathbf{x}_n \in \mathbb{C}^{L \times 1}$, and sends it according to the following transmit power constraint:

$$\mathbb{E} \{ \mathbf{x}_n^H \mathbf{x}_n \} \leq P_n^{\text{Max}} \quad \forall n \in \mathcal{N}, \quad (1)$$

where P_n^{Max} is the maximum transmit power available at BS n .

Let $\mathbf{h}_{n,k} \in \mathbb{C}^{L \times 1}$ denote the channel vector between BS n and user k , and $\mathbf{h}_k = [\mathbf{h}_{1,k}^T, \mathbf{h}_{2,k}^T, \dots, \mathbf{h}_{N,k}^T]^T \in \mathbb{C}^{NL \times 1}$ be the aggregate channel vector of user k . We can write the received signal at user k as

$$y_k = \mathbf{h}_k^H \mathbf{x} + n_k \quad (2)$$

where, $n_k \sim \mathcal{CN}(0, \sigma^2)$ is the additive white Gaussian noise (AWGN), and $\mathbf{x} = [\mathbf{x}_1^T, \dots, \mathbf{x}_N^T]^T$.

For mathematical tractability, the paper assumes that the CP has complete knowledge of the instantaneous channel state information (CSI) of all BSs. We further adopt a block-based transmission model, where each transmission block consists of several time slots. The channel fading coefficients remain constant within one block, but may vary independently from one block to another. Next, we describe our proposed scheme which is based on RS-CMD, and we formulate the WSR optimization problem accordingly.

III. TRANSMISSION SCHEME AND PROBLEM FORMULATION

The proposed transmission scheme consists of RS, joint beamforming and data-sharing, and successive common message decoding. We start by describing RS.

A. Rate Splitting

The CP first splits the message of user k , i.e., v_k , into a private message denoted by v_k^p , and a common message denoted by v_k^c . Afterwards, the CP encodes the private and common messages into s_k^p and s_k^c , respectively, as illustrated in Fig. 1. The coded messages s_k^p and s_k^c are assumed to be i.i.d. circularly symmetric complex Gaussian with zero mean and unit variance. Their respective rates are denoted by R_k^p and R_k^c , and so $R_k = R_k^p + R_k^c$, where R_k is the rate of user k .

B. Beamforming, Signal Construction, and Data-Sharing

When adopting the data-sharing strategy in a downlink mode in C-RAN which applies RS-CMD, the CP shares the encoded private and common messages directly with their respective cluster of BSs. Let $\mathcal{K}_n^p, \mathcal{K}_n^c \subseteq \mathcal{K}$ be the subset of users served by BS n with a private or common message, respectively, i.e.,

$$\mathcal{K}_n^p := \{k \in \mathcal{K} \mid \text{BS } n \text{ delivers } s_k^p \text{ to user } k\}, \quad (3)$$

$$\mathcal{K}_n^c := \{k \in \mathcal{K} \mid \text{BS } n \text{ delivers } s_k^c \text{ to user } k\}. \quad (4)$$

Moreover, let the beamformers used by BS n to send s_k^p and s_k^c to user k be denoted by $\mathbf{w}_{n,k}^p$ and $\mathbf{w}_{n,k}^c$, respectively. Then, the CP sends $\{s_k^p \mid \forall k \in \mathcal{K}_n^p\}$, $\{s_k^c \mid \forall k \in \mathcal{K}_n^c\}$ and their beamforming vectors over the backhaul links to BS n . Due to the finite backhaul capacity C_n limits, the transmission rate is subject to the following backhaul capacity constraint¹:

$$\sum_{k \in \mathcal{K}_n^p} R_k^p + \sum_{k \in \mathcal{K}_n^c} R_k^c \leq C_n, \quad \forall n \in \mathcal{N} \quad (5)$$

BS n then constructs \mathbf{x}_n as follows:

$$\mathbf{x}_n = \sum_{k \in \mathcal{K}_n^p} \mathbf{w}_{n,k}^p s_k^p + \sum_{k \in \mathcal{K}_n^c} \mathbf{w}_{n,k}^c s_k^c. \quad (6)$$

Using the expression of the transmit signal (6), one can rewrite the power constraint (1) as follows:

$$\sum_{k \in \mathcal{K}} \left(\|\mathbf{w}_{n,k}^p\|_2^2 + \|\mathbf{w}_{n,k}^c\|_2^2 \right) \leq P_n^{\text{Max}}, \quad \forall n \in \mathcal{N}. \quad (7)$$

¹We ignore the overhead due to sending the beamformers since these need to be sent only when CSI changes.

The private (common) message of user k is served by BS n , if the corresponding beamforming vector $\mathbf{w}_{n,k}^p$ ($\mathbf{w}_{n,k}^c$) is non-zero. This can be equivalently expressed in terms of the indicator function as follows:

$$\mathbb{1} \left\{ \|\mathbf{w}_{n,k}^o\|_2^2 \right\} = \begin{cases} 1 & \text{if } \|\mathbf{w}_{n,k}^o\|_2^2 > 0 \\ 0 & \text{otherwise} \end{cases} \quad (8)$$

where, $o \in \{p, c\}$. Without loss of generality, the above indicator function can be written as a function of an l_0 -norm notation², i.e., as $\mathbb{1} \left\{ \|\mathbf{w}_{n,k}^o\|_2^2 \right\} = \left\| \|\mathbf{w}_{n,k}^o\|_2^2 \right\|_0$. This is this case since, in the scalar case, the l_0 -norm definition coincides with the definition of the indicator function, because the power transmitted from BS n to user k is a positive scalar, i.e., $\|\mathbf{w}_{n,k}^o\|_2^2 \in \mathbb{R}_+$. The subset of users served with private and common messages from BS n can, therefore, be expressed as:

$$\mathcal{K}_n^p = \left\{ k \mid \left\| \|\mathbf{w}_{n,k}^p\|_2^2 \right\|_0 = 1 \right\}, \quad (9)$$

$$\mathcal{K}_n^c = \left\{ k \mid \left\| \|\mathbf{w}_{n,k}^c\|_2^2 \right\|_0 = 1 \right\}. \quad (10)$$

The above expressions allow to re-express the backhaul constraint (5) in the following compact form:

$$\sum_{k \in \mathcal{K}} \left(\left\| \|\mathbf{w}_{n,k}^p\|_2^2 \right\|_0 R_k^p + \left\| \|\mathbf{w}_{n,k}^c\|_2^2 \right\|_0 R_k^c \right) \leq C_n \quad \forall n \in \mathcal{N}. \quad (11)$$

C. Successive Decoding

At this step, the received signal at user k can be written as

$$y_k = \mathbf{h}_k^H (\mathbf{w}_k^p s_k^p + \mathbf{w}_k^c s_k^c) + \sum_{j \in \mathcal{K} \setminus \{k\}} \mathbf{h}_k^H (\mathbf{w}_j^p s_j^p + \mathbf{w}_j^c s_j^c) + n_k,$$

where $\mathbf{w}_k^p = [(\mathbf{w}_{1,k}^p)^T, \dots, (\mathbf{w}_{N,k}^p)^T]^T$ is the aggregate beamforming vector associated with s_k^p , i.e., the private message of user k . Similarly, \mathbf{w}_k^c is the aggregate beamforming vector associated with s_k^c , i.e., the common message of user k .

In the context of this paper, using common messages is adopted for the sole purpose of mitigating interference in CRANs. Thus, the order in which user k decodes the intended messages plays an important role in assessing the efficiency of the relevant proposed interference mitigation techniques. Although joint decoding of all common and private messages at user k would result

² l_0 -norm of a vector is the number of non-zero elements in this vector.

in optimized rates, its implementation is complicated in practice, in particular when the network and the intended set of messages to be decoded by each user are large. The classical information theoretical results of a 2-user IC, however, already suggest that decoding a strong interferer's common message can significantly improve a user's achievable rate [15]. From this perspective, in this paper, we focus on a successive decoding strategy, wherein user k decodes a subset of all common messages in a fixed decoding strategy, based on the descending order of the channel gains of the interferers, as described next.

Let \mathcal{M}_k denote set of users who would decode s_k^c , i.e.:

$$\mathcal{M}_k := \{j \in \mathcal{K} \mid \text{user } j \text{ decodes } s_k^c\}. \quad (12)$$

The set of common messages that user k would decode is then defined as:

$$\Phi_k := \{j \in \mathcal{K} \mid k \in \mathcal{M}_j\}. \quad (13)$$

We note that once the set \mathcal{M}_k is found, we can determine the set Φ_k , and vice-versa. The choice of Φ_k (and consequently \mathcal{M}_k) has a crucial impact on the achievable rate of user k . In this paper, we design Φ_k (and \mathcal{M}_k) in a heuristic fashion, which is based on the order of the interfering channel gains.

Consider the following decoding order at user k :

$$\pi_k(j) : \Phi_k \rightarrow \{1, 2, \dots, |\Phi_k|\},$$

i.e., $\pi_k(j)$ is the successive decoding step in which the message $j \in \Phi_k$ is decoded at user k . In other terms, $\pi_k(j_1) > \pi_k(j_2)$ (where $j_1 \neq j_2$) implies that user k decodes the common message of user j_1 first, and then the common message of user j_2 . Now, write \mathbf{y}_k , the received signal at user k , as follows,

$$\begin{aligned} y_k = & \underbrace{\left(\mathbf{h}_k^H \mathbf{w}_k^p s_k^p + \sum_{j \in \Phi_k} \mathbf{h}_k^H \mathbf{w}_j^c s_j^c \right)}_{\text{Signals to be decoded}} \\ & + \underbrace{\sum_{j \in \mathcal{K} \setminus k} \mathbf{h}_k^H \mathbf{w}_j^p s_j^p + \sum_{l \in \mathcal{K} \setminus \Phi_k} \mathbf{h}_k^H \mathbf{w}_l^c s_l^c}_{\text{Interference plus noise}} + n_k. \end{aligned} \quad (14)$$

Since finding the optimal decoding order is obviously a challenging problem for its combinatorial

nature, we herein propose a practical successive decoding strategy instead. The idea is to fix the decoding order according to channel strength in descending order as follows: $\|\mathbf{h}_{\pi_k(1)}\| \geq \|\mathbf{h}_{\pi_k(2)}\| \geq \dots \geq \|\mathbf{h}_{\pi_k(|\Phi_k|)}\|$. Such decoding strategy helps the users whose common messages are decoded achieving better common rates. Although the proposed decoding technique does not provide the global optimal solution to the problem, the simulations section of the paper later illustrate how that such a decoding order indeed provides an appreciable gain as compared to the conventional private-information transmission only, i.e., TIN.

D. Achievable Rate

Let $\Gamma_k^p, \Gamma_{k,i}^c$ denote the signal to interference plus noise ratios (SINR's) of user k , when decoding its private message and the common message of user i , respectively. Based on equation (14), we can write:

$$\Gamma_k^p = \frac{|\mathbf{h}_k^H \mathbf{w}_k^p|^2}{\sum_{j \in \mathcal{K} \setminus k} |\mathbf{h}_k^H \mathbf{w}_j^p|^2 + \sum_{l \in \mathcal{K} \setminus \Phi_k} |\mathbf{h}_k^H \mathbf{w}_l^c|^2 + \sigma^2} \quad (15)$$

$$\Gamma_{k,i}^c = \frac{|\mathbf{h}_k^H \mathbf{w}_i^c|^2}{T_k + \sum_{l \in \mathcal{K} \setminus \Phi_k} |\mathbf{h}_k^H \mathbf{w}_l^c|^2 + \sum_{\substack{m \in \Phi_k \\ \pi_k(m) > \pi_k(i)}} |\mathbf{h}_k^H \mathbf{w}_m^c|^2} \quad (16)$$

where $T_k = \sum_{j \in \mathcal{K}} |\mathbf{h}_k^H \mathbf{w}_j^p|^2 + \sigma^2$. The above expressions (15) and (16) assume that each user decodes its private message last, which is adopted for its capability to reduce the interference through common message decoding, as in the classical multi-cell systems [21]. The total achievable rate of user k , $R_k = R_k^p + R_k^c$, then satisfies the following achievability conditions:

$$\Gamma_k^p \geq 2^{R_k^p/B} - 1, \quad \forall k \in \mathcal{K}, \quad (17)$$

$$\Gamma_{i,k}^c \geq 2^{R_k^c/B} - 1, \quad \forall i \in \mathcal{M}_k \text{ and } \forall k \in \mathcal{K}. \quad (18)$$

E. Determining the Common Message Sets

The latest results of TIN in interference networks, e.g., [33], suggest a scheduling procedure to manage interfering links in a device-to-device (D2D) network. The idea in [33] is to allow the links which meet the TIN optimality criteria to share the same resources block (bandwidth, transmit frequency). Optimality of TIN criteria is then illustrated in terms of generalized degrees-of-freedom. In short, if a link causes much interference to other links (already scheduled to a

transmitting resource block), or suffers from much interference, then one should schedule it to another block.

In the context of our paper, instead of scheduling users to other transmitting blocks, we propose to deploy RS-CMD strategy for the users which cause high levels of interference to other users, so as to determine a heuristic, yet reasonable, strategy for determining the common message sets. To this end, we propose a simple criterion to identify the users which receive too much interference (weak users), and allow them to decode the common messages of strong interferers (strong users). The network we are interested in is more complex than those studied in [33]–[35]. The proposed criterion, although being a heuristic one, leads to a significant gain over the TIN strategy used in the state-of-the art C-RAN, as illustrated later in the simulations section.

Our proposed algorithm relies on first identifying the users for which TIN is not optimal, i.e., solely based on their channel gains. We do so by initializing the beamformers of all users as feasible maximum ratio combining (MRC) beamformers. Then we compute the achievable rates, and for each user, we evaluate the total interference received from other users. To best identify whether a user is considered a weak or a strong interferer, we define a parameter μ as a separating threshold. More specifically, if the rate of a user k is within the μ th percentile, the user is considered a weak user, and the L -th strongest interferers of user k are added to the set Φ_k , where L is the number of antennas of each base-station. We note that μ plays an important role in bridging the gap between RS with RS-CMD. In other terms, when μ is small, only the weakest users would decode the common message of their interferers. By increasing μ , however, more users participate in decoding the common messages of their interferers, which adds more constraints to the optimization problem; thereby reducing the value of the optimized objective function, as the simulation results later suggest.

The above strategy guarantees that user k would mitigate the interference it receives by decoding the common message of the strongest interferer. The intuition behind this is that, if the rate of a user k is high relative to other weakest users, this user would not be receiving a high level of interference, which makes it less useful that user k would decode the common message of other users. The steps of determining the set of common messages for all users $k \in \mathcal{K}$ are summarized in Algorithm 1 description below.

Algorithm 1 Procedure to Identify $\{\Phi_k\}_{k=1}^K$

```

1: Input: CSI matrix  $\mathbf{H}$ , set of active users  $\mathcal{K}$  and initialize  $\{\Phi_k = \{k\}\}_{k=1}^K$ .
2: Compute the beamformers as  $\mathbf{W} = \mathbf{H}^H$ .
3: Compute the achievable rates using TIN, based on step 2,.
4: for  $k \in \mathcal{K}$  do
5:    $\hat{\mathcal{K}} \leftarrow \mathcal{K} \setminus \{k\}$ 
6:   Compute the interference power  $\{I_{k,i}\}_{i \in \hat{\mathcal{K}}}$  as observed at user  $k$ .
7:
8:   if  $R_k$  is within the  $\mu$ -th percentile of other users rate then
9:      $\Phi_k = \Phi_k \cup \left\{ \underset{i \in \hat{\mathcal{K}}}{\operatorname{argmax}} I_{k,i} \right\}$ 
10:     $\hat{\mathcal{K}} \leftarrow \hat{\mathcal{K}} \setminus \left\{ \underset{i \in \hat{\mathcal{K}}}{\operatorname{argmax}} I_{k,i} \right\}$ 
11:    if  $|\Phi_k| > L$  then
12:       $\mathcal{K} \leftarrow \mathcal{K} \setminus \{k\}$ 
13:    end if
14:  end if
15: end for

```

F. Weighted Sum-Rate Maximization

The optimization problem considered in this paper focuses on maximizing the weighted sum-rate (WSR) in RS-CMD C-RAN. The goal is to determine the common and private beamformers jointly with the common and private clusters of BSs associated with each user, subject to per BS transmission power and backhaul constraints. The considered WSR maximization problem can be mathematically written as:

$$\underset{\{\mathbf{w}_k^p, \mathbf{w}_k^c | \forall k \in \mathcal{K}\}}{\text{maximize}} \quad \sum_{k=1}^K \alpha_k (R_k^p + R_k^c) \quad (19a)$$

$$\text{subject to} \quad (7), (11) \quad (19b)$$

$$\Gamma_k^p \geq 2^{R_k^p/B} - 1 \quad \forall k \in \mathcal{K} \quad (19c)$$

$$\Gamma_{i,k}^c \geq 2^{R_k^c/B} - 1 \quad \forall i \in \mathcal{M}_k \text{ and } \forall k \in \mathcal{K} \quad (19d)$$

where the coefficient α_k refers to the priority weight associated with user k . Problem (19) is a mixed integer non linear problem, which is generally an NP-hard problem, due to its mixed discrete and continuous optimization nature, and the non-convexity of the underlying constraints. To tackle this challenging problem, we propose an iterative algorithm based on a strongly inner-

convex approximation framework coupled with a smooth approximation of the non-smooth, non-convex l_0 -norm. Before we proceed to the technical details of our approach, we elaborate on the structure of problem (19). The problem is non-convex even if we relax the binary constraints in (11), e.g., by using l_1 relaxation to the l_0 -norm. This is due to non-convexity of the objective (19a) as a function of the beamforming vectors. Moreover, the achievability constraints and the backhaul constraints in (19c)-(19d) and (11) are non-convex functions, and define a non-convex feasible set. To overcome this difficulty, we approximate each non-convex function with a surrogate upper-bound convex function, which helps approximating the non-convex feasible set with a convex one. Then, we iteratively refine this approximation till convergence. The following section describes all the technicalities of the above steps in details.

IV. PROPOSED SOLUTION

In this section, we present our proposed framework to tackle problem (19). We start by relaxing the discrete variables, and then we proceed by introducing the ICA reformulation of the non-convex clustering problem. After determining the clusters, we determine the optimal beamforming vectors and the RS mode to transmit private and common messages, respectively, which also quantifies how much rate is assigned to the private and common messages, respectively.

A. Relaxing the l_0 -norm

We use a smooth concave function to approximate the non-smooth, non-convex (in fact integer) l_0 -norm. Consider the function $f_\theta(x)$ defined as:

$$f_\theta(x) = \frac{2}{\pi} \arctan\left(\frac{x}{\theta}\right), \quad x \geq 0 \quad (20)$$

which is often used in the literature to approximate the l_0 -norm [10], [36]. Here, θ is a smoothness parameter which controls the quality of the l_0 -norm approximation. After relaxing the discrete l_0 -norm, we reformulate the problem (19) by introducing SINR variables instead of using the rate expressions. Let $R_k^p = B \log_2(1 + \gamma_k^p)$ and $R_k^c = B \log_2(1 + \gamma_k^c)$ for some $\gamma_k^p, \gamma_k^c > 0$. Now,

we can rewrite (19) as:

$$\begin{aligned} & \underset{\{\mathbf{w}_k^p, \mathbf{w}_k^c, \gamma_k | \forall k \in \mathcal{K}\}}{\text{maximize}} && \sum_{k=1}^K \alpha_k B(\log_2(1 + \gamma_k^p) + \log_2(1 + \gamma_k^c)) \\ & \text{subject to} && (7) \end{aligned} \quad (21a)$$

$$\Gamma_k^p \geq \gamma_k^p \quad \forall k \in \mathcal{K} \quad (21b)$$

$$\Gamma_{i,k}^c \geq \gamma_k^c \quad \forall i \in \mathcal{M}_k \text{ and } \forall k \in \mathcal{K} \quad (21c)$$

$$\sum_{k \in \mathcal{K}} B\left(f_\theta\left(\|\mathbf{w}_{n,k}^p\|_2^2\right) \log_2(1 + \gamma_k^p) + f_\theta\left(\|\mathbf{w}_{n,k}^c\|_2^2\right) \log_2(1 + \gamma_k^c)\right) \leq C_n \quad \forall n \in \mathcal{N}. \quad (21d)$$

Problem (21) is still non-convex despite relaxing the binary constraints. This is because the feasible set defined by constraints (21b)-(21d) is a non-convex set. To overcome this challenge, we use some algebraic manipulations to rewrite the problem (21) in a form that is easier to tackle, as described next in the text.

B. Clustering

Given the SINR expressions in (15) and (16), we can equivalently write the constraints (21b) and (21c) as:

$$\sum_{j \in \mathcal{K} \setminus k} |\mathbf{h}_k^H \mathbf{w}_j^p|^2 + \sum_{l \in \mathcal{K} \setminus \Phi_k} |\mathbf{h}_k^H \mathbf{w}_l^c|^2 + \sigma^2 - \frac{|\mathbf{h}_k^H \mathbf{w}_k^p|^2}{\gamma_k^p} \leq 0 \quad (22)$$

$$T_k + \sum_{l \in \mathcal{K} \setminus \Phi_k} |\mathbf{h}_k^H \mathbf{w}_l^c|^2 + \sum_{\substack{m \in \Phi_k \\ \pi_k(m) > \pi_k(i)}} |\mathbf{h}_k^H \mathbf{w}_m^c|^2 - \frac{|\mathbf{h}_k^H \mathbf{w}_k^c|^2}{\gamma_k^c} \leq 0 \quad (23)$$

Note that the function $\frac{|\mathbf{h}_k^H \mathbf{w}_k^p|^2}{\gamma_k^p}$ in (22) is of the form $\frac{\|x\|_2^2}{\beta}$, which is a convex quadratic function [36]–[38]. This reformulation is useful, because it converts the constraints (21b) and (21c) to a difference of convex functions, which facilitates the inner-convex approximation. Let $\mathbf{t}_k = [t_{1,k}^p, t_{1,k}^c, \dots, t_{N,k}^p, t_{N,k}^c]^T$ and $\mathbf{d}_k = [d_k^p, d_k^c]$ be slack variables. With the help of such new variables \mathbf{t}_k and \mathbf{d}_k , rewrite the optimization problem (21) by splitting the constraint in (21d) into five

simpler constraints as follows:

$$\begin{aligned} & \underset{\{\mathbf{w}_k^p, \mathbf{w}_k^c, \gamma_k, \mathbf{d}_k, \mathbf{t}_k | \forall k \in \mathcal{K}\}}{\text{maximize}} && \sum_{k=1}^K g_1(\gamma_k^p, \gamma_k^c) \end{aligned} \quad (24a)$$

$$\text{subject to} \quad (7), (22) - (23) \quad (24b)$$

$$\sum_{k \in \mathcal{K}} (t_{n,k}^p d_k^p + t_{n,k}^c d_k^c) \leq C_n/B \quad \forall n \in \mathcal{N} \quad (24c)$$

$$f_\theta \left(\|\mathbf{w}_{n,k}^p\|_2^2 \right) \leq t_{n,k}^p \text{ and } f_\theta \left(\|\mathbf{w}_{n,k}^c\|_2^2 \right) \leq t_{n,k}^c \quad (24d)$$

$$\log_2(1 + \gamma_k^p) \leq d_k^p \quad (24e)$$

$$\log_2(1 + \gamma_k^c) \leq d_k^c \quad \forall n \in \mathcal{N} \text{ and } \forall k \in \mathcal{K} \quad (24f)$$

where the function $g_1(\gamma_k^p, \gamma_k^c)$ is defined as: $g_1(\gamma_k^p, \gamma_k^c) = \alpha_k B (\log_2(1 + \gamma_k^p) + \log_2(1 + \gamma_k^c))$. The following proposition illustrates how problems (21) and (24) are indeed equivalent to each other.

Proposition 1. (\mathbf{w}^*, γ^*) is a stationary solution of (21) if and only if there exist $(\mathbf{t}^*, \mathbf{d}^*)$ such that $(\mathbf{w}^*, \gamma^*, \mathbf{t}^*, \mathbf{d}^*)$ is a stationary solution of (24).

Proof. The respective formulations of problems (21) and (24) share the same objective function. Moreover, the maximum transmit power constraint (7) is the same in both problems. Constraints in (22)–(23) are equivalent mathematical manipulations of constraints (21b)–(21c). Furthermore, constraint (21d) is equivalent to constraints (24c)–(24f), after introducing the slack variables \mathbf{t}, \mathbf{d} . Therefore, optimization problems (21) and (24) are equivalent to each other. \square

Solving problem (24) helps finding the clusters which serve the private and common messages respectively for each user. But since (24) is a non-convex problem, we propose using inner-convex approximation (ICA), so as to approximate the non-convex feasible set of problem (24) as described next.

C. Inner Convex Approximations (ICA)

Although problem (24) is a non-convex problem, this paper adopts well-chosen ICA techniques to convexify its feasibility set, which is defined by constraints in (24b)–(24f). We start with some

algebraic transformations to constraint (24c). We note that the bilinear function $t_{n,k}^p d_k^p + t_{n,k}^c d_k^c$ can be equivalently written as

$$t_{n,k}^p d_k^p + t_{n,k}^c d_k^c = \frac{1}{2} \sum_{o \in \{p,c\}} [(t_{n,k}^o + d_k^o)^2 - (t_{n,k}^o)^2 - (d_k^o)^2] \quad (25)$$

This form is equivalent to a convex plus concave functions (difference of two convex functions). We proceed by introducing a convex upper bound to the bilinear function in (25), by keeping the convex part and replacing the concave function with its first-order approximation.

Let $\tilde{g}_2(\mathbf{t}, \mathbf{d}, \tilde{\mathbf{t}}, \tilde{\mathbf{d}})$ be defined as:

$$\begin{aligned} \tilde{g}_2(\mathbf{t}, \mathbf{d}, \tilde{\mathbf{t}}, \tilde{\mathbf{d}}) \triangleq & \sum_{k \in \mathcal{K}} \sum_{o \in \{p,c\}} \left(\frac{1}{2} (t_{n,k}^o + d_k^o)^2 - \frac{1}{2} (\tilde{t}_{n,k}^o)^2 \right. \\ & - \frac{1}{2} (\tilde{d}_k^o)^2 - \tilde{t}_{n,k}^o (t_{n,k}^o - \tilde{t}_{n,k}^o) \\ & \left. - \tilde{d}_k^o (d_k^o - \tilde{d}_k^o) \right) - C_n/B \quad \forall n \in \mathcal{N} \end{aligned} \quad (26)$$

where, $(\tilde{\mathbf{t}}, \tilde{\mathbf{d}})$ are feasible fixed values, which satisfy constraints (24c)–(24f).

Proposition 2. For any feasible vectors $(\tilde{\mathbf{t}}, \tilde{\mathbf{d}})$, the function $\tilde{g}_2(\mathbf{t}, \mathbf{d}, \tilde{\mathbf{t}}, \tilde{\mathbf{d}})$ is a valid surrogate of the constraint in (24c) and satisfies:

$$\tilde{g}_2(\mathbf{t}, \mathbf{d}, \tilde{\mathbf{t}}, \tilde{\mathbf{d}}) \geq \underbrace{\sum_{k \in \mathcal{K}} (t_{n,k}^p d_k^p + t_{n,k}^c d_k^c)}_{g_2(\mathbf{t}, \mathbf{d})} - C_n/B \quad (27)$$

for all feasible values $(\tilde{\mathbf{t}}, \tilde{\mathbf{d}})$.

Proof. We note that the function

$$g_{n,k}(\mathbf{y}) \triangleq \frac{1}{2} \sum_{o \in \{p,c\}} \left[\underbrace{(t_{n,k}^o + d_k^o)^2}_{g_{n,k,o}^+(\mathbf{y})} - \underbrace{((t_{n,k}^o)^2 + (d_k^o)^2)}_{g_{n,k,o}^-(\mathbf{y})} \right] \quad (28)$$

has a structure of difference of two convex functions, where both functions $g_{n,k,o}^+(\mathbf{y})$ and $g_{n,k,o}^-(\mathbf{y})$ are convex, and $\mathbf{y} = [\mathbf{t}^T, \mathbf{d}^T]^T$. By keeping the convex part $g_{n,k,o}^+(\cdot)$ unchanged and linearising the concave part $-g_{n,k,o}^-(\cdot)$ using the first order approximation around the point $(\tilde{t}_{n,k}^o, \tilde{d}_k^o) \forall o \in \{p, c\}$, we get the following convex upper approximation of the function $g_{n,k}(\mathbf{y})$:

$$\tilde{g}_{n,k}(\mathbf{y}, \tilde{\mathbf{y}}) \triangleq \frac{1}{2} \sum_{o \in \{p,c\}} g_{n,k,o}^+(\mathbf{y}) - g_{n,k,o}^-(\tilde{\mathbf{y}}) - \nabla_{\mathbf{y}} g_{n,k,o}^-(\tilde{\mathbf{y}})^T (\mathbf{y} - \tilde{\mathbf{y}}), \quad (29)$$

where $\tilde{\mathbf{y}} = [\tilde{\mathbf{t}}^T, \tilde{\mathbf{d}}^T]^T$.

We can write the function $\tilde{g}_{n,k}(\mathbf{y}, \tilde{\mathbf{y}})$ as

$$\tilde{g}_{n,k}(\mathbf{y}, \tilde{\mathbf{y}}) =: \sum_{o \in \{p,c\}} \left(\frac{1}{2} (t_{n,k}^o + d_k^o)^2 - \frac{1}{2} (\tilde{t}_{n,k}^o)^2 - \frac{1}{2} (\tilde{d}_k^o)^2 - \tilde{t}_{n,k}^o (t_{n,k}^o - \tilde{t}_{n,k}^o) - \tilde{d}_k^o (d_k^o - \tilde{d}_k^o) \right) \quad (30)$$

Based on the convexity of $g_{n,k}^-(\mathbf{y})$, the following inequality follows: $t_{n,k}^p d_k^p + t_{n,k}^c d_k^c = g_{n,k}(\mathbf{y}) \leq \tilde{g}_{n,k}(\mathbf{y}, \tilde{\mathbf{y}})$. This completes the proof of proposition 2. \square

Afterwards, we perform distinct ICA operations for the remaining constraints. More precisely, for constraint (24d), we linearize the concave functions $f_\theta \left(\|\mathbf{w}_{n,k}^p\|_2^2 \right)$ and $f_\theta \left(\|\mathbf{w}_{n,k}^c\|_2^2 \right)$ around $\tilde{\mathbf{w}}_{n,k}^p$ and $\tilde{\mathbf{w}}_{n,k}^c$, respectively. This leads to the following inner-convex approximation of the set defined by the constraints in (24d):

$$\tilde{g}_3(\mathbf{w}_{n,k}^p, \tilde{\mathbf{w}}_{n,k}^p) \triangleq f_\theta \left(\|\mathbf{w}_{n,k}^p\|_2^2 \right) + \nabla f_\theta \left(\|\mathbf{w}_{n,k}^p\|_2^2 \right) \left(\|\mathbf{w}_{n,k}^p\|_2^2 - \|\tilde{\mathbf{w}}_{n,k}^p\|_2^2 \right) \quad (31)$$

$$\tilde{g}_4(\mathbf{w}_{n,k}^c, \tilde{\mathbf{w}}_{n,k}^c) \triangleq f_\theta \left(\|\mathbf{w}_{n,k}^c\|_2^2 \right) + \nabla f_\theta \left(\|\mathbf{w}_{n,k}^c\|_2^2 \right) \left(\|\mathbf{w}_{n,k}^c\|_2^2 - \|\tilde{\mathbf{w}}_{n,k}^c\|_2^2 \right) \quad (32)$$

We follow the same procedure with constraints (24e) and (24f), where we linearize the concave functions $\log_2(1 + \gamma_k^p)$, $\log_2(1 + \gamma_k^c)$ around $\tilde{\gamma}_k^p$ and $\tilde{\gamma}_k^c$, respectively. We obtain the following equations which define an inner-convex approximation of the non-convex feasible set defined by constraints (24e) and (24f):

$$\tilde{g}_5(\gamma_k^p, \tilde{\gamma}_k^p) \triangleq \log_2(1 + \tilde{\gamma}_k^p) + \frac{1}{(1 + \tilde{\gamma}_k^p) \ln(2)} (\gamma_k^p - \tilde{\gamma}_k^p) \leq 0 \quad (33)$$

$$\tilde{g}_6(\gamma_k^c, \tilde{\gamma}_k^c) \triangleq \log_2(1 + \tilde{\gamma}_k^c) + \frac{1}{(1 + \tilde{\gamma}_k^c) \ln(2)} (\gamma_k^c - \tilde{\gamma}_k^c) \leq 0 \quad (34)$$

Concerning the SINR constraints in (22) and (23), we note that if $(\tilde{\mathbf{w}}, \tilde{\gamma})$ is a feasible point of (24), then the following holds:

$$\frac{|\mathbf{h}_k^H \mathbf{w}_k^p|^2}{\gamma_k^p} \geq \frac{2\Re \left\{ (\tilde{\mathbf{w}}_k^p)^H \mathbf{h}_k \mathbf{h}_k^H \mathbf{w}_k^p \right\}}{\tilde{\gamma}_k^p} - \frac{|\mathbf{h}_k^H \tilde{\mathbf{w}}_k^p|^2}{(\tilde{\gamma}_k^p)^2} \gamma_k^p \quad (35)$$

and

$$\frac{|\mathbf{h}_i^H \mathbf{w}_k^c|^2}{\gamma_k^c} \geq \frac{2\Re \left\{ (\tilde{\mathbf{w}}_k^c)^H \mathbf{h}_i \mathbf{h}_i^H \mathbf{w}_k^c \right\}}{\tilde{\gamma}_k^c} - \frac{|\mathbf{h}_i^H \tilde{\mathbf{w}}_k^c|^2}{(\tilde{\gamma}_k^c)^2} \gamma_k^c \quad (36)$$

where, $\Re \{ \cdot \}$ is the real part of a complex number. Based on inequalities (35) and (36), we can

establish inner-convex approximations of the constraints in (22) and (23) as follows:

$$\tilde{g}_7(\mathbf{w}, \gamma_k^p; \tilde{\mathbf{w}}, \tilde{\gamma}_k^p) \triangleq \sum_{j \in \mathcal{K} \setminus k} |\mathbf{h}_k^H \mathbf{w}_j^p|^2 + \sum_{l \in \mathcal{K} \setminus \Phi_k} |\mathbf{h}_k^H \mathbf{w}_l^c|^2 + \sigma^2 - \frac{2\Re\left\{(\tilde{\mathbf{w}}_k^p)^H \mathbf{h}_k \mathbf{h}_k^H \mathbf{w}_k^p\right\}}{\tilde{\gamma}_k^p} + \frac{|\mathbf{h}_k^H \tilde{\mathbf{w}}_k^p|^2}{(\tilde{\gamma}_k^p)^2} \gamma_k^p \quad (37)$$

$$\begin{aligned} \tilde{g}_8(\mathbf{w}, \gamma_k^c; \tilde{\mathbf{w}}, \tilde{\gamma}_k^c) \triangleq & T_k + \sum_{l \in \mathcal{K} \setminus \Phi_k} |\mathbf{h}_k^H \mathbf{w}_l^c|^2 + \sum_{\substack{m \in \Phi_k \\ \pi_k(m) > \pi_k(i)}} |\mathbf{h}_k^H \mathbf{w}_m^c|^2 + \frac{|\mathbf{h}_i^H \tilde{\mathbf{w}}_k^c|^2}{(\tilde{\gamma}_k^c)^2} \gamma_k^c \\ & - \frac{2\Re\left\{(\tilde{\mathbf{w}}_k^c)^H \mathbf{h}_i \mathbf{h}_i^H \mathbf{w}_k^c\right\}}{\tilde{\gamma}_k^c} \end{aligned} \quad (38)$$

Now we are ready to present the strongly inner-convex approximations of problem (21) and the algorithm to solve it.

D. Strongly ICA based Algorithm

The functions in (26),(31)–(34) and (37)–(38) define a convex feasible set, which represents an inner-approximation of the non-convex feasible set of problem (24). The idea of our approach is to iteratively solve the optimization problem defined with this approximation. After each iteration, we refine the ICA of the feasible set in (24), and keep iterating until convergence to a stationary solution, as described next. The approximate optimization problem is defined as follows:

$$\begin{aligned} & \text{maximize} && \sum_{k=1}^K g_1(\gamma_k^p, \gamma_k^c) - g_9(\mathbf{w}, \gamma; \tilde{\mathbf{w}}, \tilde{\gamma}) \\ & \{\mathbf{w}_k^p, \mathbf{w}_k^c, \gamma_k, \mathbf{d}_k, \mathbf{t}_k | \forall k \in \mathcal{K}\} \end{aligned} \quad (39a)$$

$$\text{subject to} \quad (7) \quad (39b)$$

$$\tilde{g}_2(t_{n,k}^i, d_{n,k}^i, \tilde{t}_{n,k}^i, \tilde{d}_{n,k}^i) \leq 0 \quad (39c)$$

$$\tilde{g}_3(\mathbf{w}_{n,k}^p, \tilde{\mathbf{w}}_{n,k}^p) \leq 0 \quad (39d)$$

$$\tilde{g}_4(\mathbf{w}_{n,k}^c, \tilde{\mathbf{w}}_{n,k}^c) \leq 0 \quad (39e)$$

$$\tilde{g}_5(\gamma_k^p, \tilde{\gamma}_k^p) \leq 0 \quad (39f)$$

$$\tilde{g}_6(\gamma_k^c, \tilde{\gamma}_k^c) \leq 0 \quad (39g)$$

$$\tilde{g}_7(\mathbf{w}, \gamma_k^p; \tilde{\mathbf{w}}, \tilde{\gamma}_k^p) \leq 0 \quad (39h)$$

$$\tilde{g}_8(\mathbf{w}, \gamma_k^c; \tilde{\mathbf{w}}, \tilde{\gamma}_k^c) \leq 0 \quad (39i)$$

Here, $g_9(\mathbf{w}, \gamma; \tilde{\mathbf{w}}, \tilde{\gamma})$ is a proximal term to assure that the objective is a strongly concave function and is defined as:

$$g_9(\mathbf{w}, \gamma; \tilde{\mathbf{w}}, \tilde{\gamma}) = \rho_1 \|\mathbf{w} - \tilde{\mathbf{w}}\|_2^2 + \rho_2 \|\gamma - \tilde{\gamma}\|_2^2. \quad (40)$$

Let $\mathbf{Z} = [\mathbf{w}^T, \gamma^T, \mathbf{t}^T, \mathbf{d}^T]^T$ be a vector stacking all the optimization variables of the problem (39). Let $\hat{\mathbf{Z}}_v$ be the variables computed at iteration v as the optimal solution of problem (39), and let $\tilde{\mathbf{Z}} = [\tilde{\mathbf{w}}^T, \tilde{\gamma}^T, \tilde{\mathbf{t}}^T, \tilde{\mathbf{d}}^T]^T$ be the point at which we compute the approximate solution of problem (39) at iteration v . Furthermore, let \mathcal{Z} denote the convex feasible set of problem (39) defined by constraints (39b)–(39i). The algorithm starts by initializing the vector $\tilde{\mathbf{Z}}$, around which we compute the next iteration. The initialization process starts by computing feasible MRC beamformers for the users' messages when considering TIN scheme, and for both private and common messages when considering RS-CMD scheme. Based on this initialization, we compute the vector $\tilde{\gamma}$ using equations (15) and (16). Note that the sets $\{\Phi_k\}_{k=1}^K$ are computed using Algorithm 1. The initialization of vectors $\tilde{\mathbf{t}}, \tilde{\mathbf{d}}$ is done solving (24d)–(24f) by replacing inequalities with equalities. After solving the problem (39) at iteration v , we get the optimal values stacked in vector $\hat{\mathbf{Z}}_v$. Using $\hat{\mathbf{Z}}_v$, we compute the vector $\tilde{\mathbf{Z}}$ for the next iteration. The detailed steps of the iterative algorithm to solve problem (21) are summarized in Algorithm 2 description below. The following theorem proves that Algorithm 2 produces a stationary solution

Algorithm 2 Inner convex approximation of (21).

- 1: Initialize: $v \leftarrow 0$, $\tilde{\mathbf{Z}} \in \mathcal{Z}$, $\rho_1 > 0$, $\rho_2 > 0$, $\xi \ll 1$, $\xi \in \mathbb{R}_+$ and $\theta = \theta_v$.
 - 2: **while** $\hat{\mathbf{Z}}_v$ not a stationary solution of (21) **do**
 - 3: Solve the convex problem (39) and compute $\hat{\mathbf{Z}}_v$
 - 4: $\tilde{\mathbf{Z}} \leftarrow \tilde{\mathbf{Z}} + \beta_v (\hat{\mathbf{Z}}_v - \tilde{\mathbf{Z}})$ for some $\beta_v \in (0, 1]$
 - 5: **if** $\theta_v \geq \xi$ **then** $\theta_v = \delta \theta_v$ and $\delta \in (0, 1)$
 - 6: **end if**
 - 7: $v \leftarrow v + 1$
 - 8: **end while**
-

of problem (21)

Theorem 1. Let $\rho_1, \rho_2 > 0$, and let the step size sequence $\{\beta_v\}$ satisfy $\beta_v \in (0, 1]$, $\beta_v \rightarrow 0$, and $\sum_v \beta_v = +\infty$. Then $\{\hat{\mathbf{Z}}_v\}$, the sequence generated by Algorithm 2, is bounded, and converges to $\{\hat{\mathbf{Z}}_v^*\}$, which is a stationary solution of problem (39), such that $(\gamma^*, \mathbf{t}^*, \mathbf{d}^*) > 0$. Therefore, (according to proposition 1), (\mathbf{w}^*, γ^*) is also a stationary point of problem (21).

Proof. Here, we want to show that the objective and constraints of problem (39) satisfy the assumptions made in [39, Sec. II]. Hence, the convergence to a stationary point is guaranteed by [39, Theorem 2]. Towards this end, we show next that the function $\tilde{g}_2(\mathbf{t}, \mathbf{d}; \tilde{\mathbf{t}}, \tilde{\mathbf{d}})$ satisfies the following properties:

- C1) $\tilde{g}_2(\tilde{\mathbf{y}}, \tilde{\mathbf{y}}) = g_2(\tilde{\mathbf{y}})$
- C2) $\tilde{g}_2(\mathbf{y}, \tilde{\mathbf{y}}) \geq g_2(\mathbf{y}) \quad \forall \tilde{\mathbf{y}} \in \mathcal{Z}$
- C3) $\tilde{g}_2(\bullet, \tilde{\mathbf{y}})$ is a convex function for all $\tilde{\mathbf{y}} \in \mathcal{Z}$
- C4) $\tilde{g}_2(\bullet, \bullet)$ is a continuous function on the feasible set.
- C5) $\nabla_{\mathbf{y}} \tilde{g}_2(\tilde{\mathbf{y}}, \tilde{\mathbf{y}}) = \nabla_{\mathbf{y}} g_2(\tilde{\mathbf{y}})$
- C6) The function $\nabla_{\mathbf{y}} \tilde{g}_2(\bullet, \bullet)$ is continuous on the feasible set.

C1 is easily checked by substituting $\mathbf{y} = [\mathbf{t}^T, \mathbf{d}^T]^T$ in (26) by $\tilde{\mathbf{y}} = [\tilde{\mathbf{t}}^T, \tilde{\mathbf{d}}^T]^T$ and then comparing the result to the function $g_2(\tilde{\mathbf{y}})$ which yield the equality. C2 follows directly from proposition 2. By noting that the function $\tilde{g}_2(\bullet, \tilde{\mathbf{y}})$ with fixed $\tilde{\mathbf{y}}$ consists of a quadratic function plus a linear function C3 follows, while the function $\tilde{g}_2(\bullet, \bullet)$ is a difference of two convex functions, which proves C4. To prove C5 and C6 we have to compute the partial derivative of the function $g_2(\bullet, \tilde{\mathbf{y}})$ as follows

$$\nabla_{\mathbf{y}} \tilde{g}_2(\mathbf{y}, \tilde{\mathbf{y}}) = \begin{cases} \frac{\partial \tilde{g}_2(\bullet, \tilde{\mathbf{y}})}{\partial \mathbf{t}} & \triangleq \sum_{k \in \mathcal{K}} \sum_{o \in \{p, c\}} \left((t_{n,k}^o + d_k^o) - \tilde{t}_{n,k}^o \right) \\ \frac{\partial \tilde{g}_2(\bullet, \tilde{\mathbf{y}})}{\partial \mathbf{d}} & \triangleq \sum_{k \in \mathcal{K}} \sum_{o \in \{p, c\}} \left((t_{n,k}^o + d_k^o) - \tilde{d}_k^o \right) \end{cases} \quad (41)$$

On the other hand we get for function $g_2(\mathbf{y})$ the following

$$\nabla_{\mathbf{y}} g_2(\mathbf{y}) = \begin{cases} \frac{\partial \tilde{g}_2(\mathbf{y})}{\partial \mathbf{t}} & \triangleq \sum_{k \in \mathcal{K}} (d_k^p + d_k^c) \\ \frac{\partial \tilde{g}_2(\mathbf{y})}{\partial \mathbf{d}} & \triangleq \sum_{k \in \mathcal{K}} (t_{n,k}^p + t_{n,k}^c) \end{cases} \quad (42)$$

By substituting \mathbf{y} with $\tilde{\mathbf{y}}$ in both (41) and (42) we proof C5. C6 follows from the fact that the function $\nabla_{\mathbf{y}} \tilde{g}_2(\bullet, \bullet)$ is a bilinear one. **This completes the proof that function $\tilde{g}_2(\mathbf{t}, \mathbf{d}; \tilde{\mathbf{t}}, \tilde{\mathbf{d}})$ satisfies the properties C1 to C6. In a similar manner we can show that the rest of functions defining the feasible set of problem (39) also satisfy this technical conditions and this completes the proof.** \square

After solving problem (24) we can determine the clusters for private and common messages

as follows:

$$\mathcal{K}_n^p = \left\{ k \mid \|\mathbf{w}_{n,k}^p\|_2^2 \geq \epsilon_1 \right\}, \quad (43)$$

$$\mathcal{K}_n^c = \left\{ k \mid \|\mathbf{w}_{n,k}^c\|_2^2 \geq \epsilon_2 \right\} \quad (44)$$

E. Beamforming and RS mode Selection

Given \mathcal{K}_n^p and \mathcal{K}_n^c we can find the optimal beamformers by solving a simplified version of problem (39). Note that now the clusters are fixed, so the optimization variables are only the group sparse vectors $\{\mathbf{w}_k^p, \mathbf{w}_k^c, \gamma_k \mid \forall k \in \mathcal{K}\}$ and therefore the search space is much simpler than that of (39) and the optimization problem is easier to solve. Obviously, the sparsity of optimization variables depends on the design parameters ϵ_1 and ϵ_2 . The optimization problem with fixed clusters is given as:

$$\begin{aligned} & \underset{\{\mathbf{w}_k^p, \mathbf{w}_k^c, \gamma_k \mid \forall k \in \mathcal{K}\}}{\text{maximize}} && \sum_{k=1}^K g_1(\gamma_k^p, \gamma_k^c) - g_9(\mathbf{w}, \gamma; \tilde{\mathbf{w}}, \tilde{\gamma}) \end{aligned} \quad (45a)$$

$$\text{subject to} \quad g_{10}(\gamma_k^p, \tilde{\gamma}_k^p, \gamma_k^c, \tilde{\gamma}_k^c) \leq 0 \quad (45b)$$

$$\sum_{k \in \mathcal{K}_n^p} \|\mathbf{w}_{n,k}^p\|_2^2 + \sum_{k \in \mathcal{K}_n^c} \|\mathbf{w}_{n,k}^c\|_2^2 \leq P_n^{\text{Max}} \quad \forall n \in \mathcal{N} \quad (45c)$$

$$g_7(\mathbf{w}, \gamma_k^p; \tilde{\mathbf{w}}, \tilde{\gamma}_k^p) \leq 0 \quad (45d)$$

$$g_8(\mathbf{w}, \gamma_k^c; \tilde{\mathbf{w}}, \tilde{\gamma}_k^c) \leq 0 \quad (45e)$$

Here, $g_{10}(\gamma_k^p, \tilde{\gamma}_k^p, \gamma_k^c, \tilde{\gamma}_k^c) \leq 0$ represent the backhaul constraint, where the function $g_{10}(\cdot)$ is defined as:

$$g_{10}(\gamma_k^p, \tilde{\gamma}_k^p, \gamma_k^c, \tilde{\gamma}_k^c) \triangleq \sum_{k \in \mathcal{K}_n^p} g_5(\gamma_k^p, \tilde{\gamma}_k^p) + \sum_{k \in \mathcal{K}_n^c} g_6(\gamma_k^c, \tilde{\gamma}_k^c) - C_n/B. \quad (46)$$

We use Algorithm 3 to obtain a stationary solution (\mathbf{w}^*, γ^*) to the beamforming problem with fixed clusters.

Here, $\mathbf{Y} = [\mathbf{w}^T, \gamma^T]^T$, $\tilde{\mathbf{Y}} = [\tilde{\mathbf{w}}^T, \tilde{\gamma}^T]^T$ and \mathcal{Y} is the feasible set of problem (45). **Now that we have described the optimization algorithm, we analyze its complexity.**

F. Complexity Analysis

At each iteration of Algorithm 2 which is used to determine the clusters, we need to solve a convex problem, precisely problem (39), with a logarithm plus proximal term in the objective.

Algorithm 3 Inner convex approximation of beamforming problem with fixed clusters.

```

1: Initialize:  $v \leftarrow 0$ ,  $\tilde{\mathbf{Y}} \in \mathcal{Y}$  and  $\rho_1 > 0, \rho_2 > 0$ 
2: while  $\hat{\mathbf{Y}}_v$  not a stationary solution. do
3:   Solve the convex problem (45) and compute  $\hat{\mathbf{Y}}_v$ 
4:    $\tilde{\mathbf{Y}} \leftarrow \tilde{\mathbf{Y}} + \beta_v (\hat{\mathbf{Y}}_v - \tilde{\mathbf{Y}})$  for some  $\beta_v \in (0, 1]$ 
5:    $v \leftarrow v + 1$ 
6: end while

```

The logarithmic part can be linearised as done in equation (33). By doing so, we end up having a quadratic convex problem which can be easily cast into a second order cone programs (SOCPs), see [40] and references therein. This approximations can be solved using interior-point methods with a complexity of $\mathcal{O}(NKL)^{3.5}$ via general-purpose solvers e.g. SDPT3 or MOSEK. After clustering, we determine the beamforming vectors and the RS mode using Algorithm 3. Obviously, Algorithm 3 is much simpler than Algorithm 2. In our implementation we use MOSEK since it is more convenient for problems which can be cast into SOCPs. Let V_{\max} be the worst-case fixed number of iterations needed for the Algorithm 2 to converge. In the worst case the overall complexity of Algorithm 2 and Algorithm 3 can be computed to be $2V_{\max}(NKL)^{3.5}$. Note this is a pessimistic upper bound, since (45) is normally sparse and therefore Algorithm 3 it is much lighter than Algorithm 2 and it converges in a less number of iteration.

V. NUMERICAL RESULTS

In this section we perform an extensive set of numerical simulations to demonstrate the performance of our proposed approach. The C-RAN consists of a 7-cell wrapped-around network. In each cell there exists a BS at the center which is connected to the cloud via a limited capacity backhaul link. The simulations parameters of this network are listed in table II. To simplify discussions, we assume that all BS's are subject to the same power constraint with maximum transmission power as listed in table II. Besides, all BS's share the same backhaul constraint. In addition to the dynamic clustering algorithms with both TIN and RS-CMD, in which we jointly optimize the BSs clusters together with the beamformers, we also consider a static clustering algorithm which forms the clusters based on path-loss information only and hence the beamformers are optimized for a fixed (static) clusters. In the following we explain briefly the static TIN clustering as used in [19], and our extended version of this algorithm to fit within RS-CMD framework.

- **Static TIN:** This scheme is based on clustering procedure described in [19, Algorithm 3]. Once the clusters are fixed, we can solve problem (45) to determine the optimal beamformers.
- **Static RS-CMD:** In this case we extend the previous procedure to accommodate clusters for private and common messages for each user. Again, when the clusters are fixed we use Algorithm 3 to solve problem (45) and find the optimal private and common beamformers.

Simulation Parameters	
Network Parameter	Value
Channel Bandwidth	10 MHz
Number of Antennas	8
Maximum transmission Power	30 dBm
Antenna gain	15 dBi
Background noise	-169 dBm/Hz
Path-loss	$140.7 + 36.7 \log_{10}(d)$
Log-normal shadowing	8 dB
Rayleigh small scale fading	0 dB

Further, we assume that each user can decode only one additional common message besides its own common message. However, a common message of a user can be decoded by multiple users. This helps reducing the complexity of the receiver, by limiting the number of successive cancellation stages.

A. Impact of inter-cell distance on the performance

First, we evaluate the performance of RS-CMD scheme in C-RAN, against the state-of-the-art TIN scheme. For both schemes we consider dynamic and static clustering procedures. In case of dynamic clustering, we use Algorithm 2 and equations (43) and (44) to determine the clusters. Then, we use Algorithm 3 with few iterations, starting from the solution computed at last iteration of Algorithm 2, to compute the beamformers. In the case of fixed static clusters, we can apply Algorithm 3 directly to compute the beamformers for both TIN and RS-CMD. We consider a network in which the inter-cell distance between two neighboring BSs is 200m. Fig. 2 shows the achievable sum rate as a function of backhaul capacity when applying these schemes, where we use RS-CMD in both static and dynamic clustering with parameter values $\mu = 25$

and $\mu = 60$. The figure shows that our proposed algorithm, namely RS-CMD with dynamic clustering and $\mu = 25$ achieves the best performance against the state-of-the art TIN. Compared with static TIN, RS-CMD 25 have a significant gain up to 42.3 % at 950 Mbps backhaul capacity. In fact, from Fig. 2 we distinguish between two capacity regions. In the low backhaul capacity region the performance is mainly limited by capacity of backhaul links. In this region, due to the scarcity of backhaul resources, a carefully chosen set of users should be assigned to each BS in order to optimize the performance with the available backhaul resources. This explains, why the static clustering schemes perform poorly in this region, while the dynamic schemes achieve sum-rates close to a capacity upper bound given by $7 * C_n$. As we move towards higher backhaul capacities, we note that the sum-rate of all schemes increases. However, The gain of our approach increases as well compared to the state-of-the art schemes under both dynamic and static clustering, i.e., static TIN and dynamic TIN. As we approach the interference limited region, by increasing the backhaul capacity, the effect of RS-CMD becomes more pronounced. This is expected, since our scheme is explicitly designed to mitigate the interference, hence its performance gets better as the interference becomes the limiting factor. Interestingly, the role of dynamic clustering becomes less significant in the interference limited regime. Here, with the short inter-cell distance, it is more probable that all users have strong channel gains to nearby BSs which have enough backhaul resources in the interference limited regime. This makes the impact of clustering in this region less significant as compared to RS-CMD. Thus, from 400 Mbps onward we observe that RS-CMD with static clustering outperforms dynamic TIN. Finally, in Fig. 2 we observe that RS-CMD scheme with $\mu = 25$ performs better than RS-CMD with $\mu = 60$. To understand this, we recall that the weak users which decode the common messages of the strong interferes, increase their feasible set by eliminating the negative impact of the strong interferes. At the same time, the common rate is now subject to additional constraints, which consequently shrinks the feasible set of the common beamformers and potentially can reduce their rates. The trade-off between these two factors is mainly determined by the choice of the set of weak users, i.e., by our choice of parameter μ . We should also mention that for such a large network, it is not optimal to choose pure RS-CMD, i.e., $\mu = 100$. Since when interference is weak between a subset of users, then TIN is optimal. In Fig. 3, we repeat our simulations for a different network in which the inter-cell distance is now 400 m. In this case, the cell-edge users are more susceptible to interference from BSs in neighboring cells. On the other hand, the users located near a cell center have better channel gains to BSs in their cell and

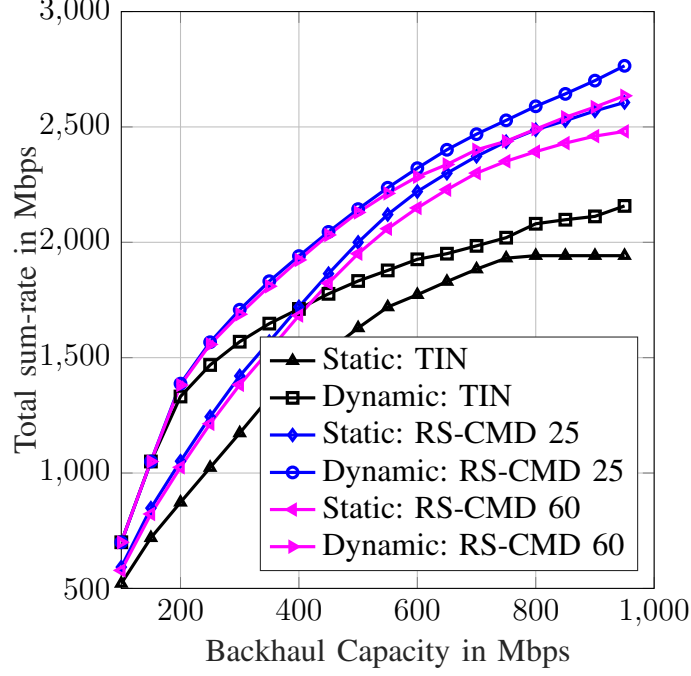


Figure 2: The performance of all studied schemes for a C-RAN with 7 BSs serving 28 users and an inter-cell distance of 200 m

weak interference channels to other BSs in other cells. Obviously, the size of clusters in this case is smaller, because only few BSs have strong channel gains to each user as compared to the previous case. This explains why all schemes perform well in the backhaul limited regime. However, as we approach the interference limited regime the impact of clustering and RS-CMD becomes more significant. In this network, RS-CMD with $\mu = 25$ achieves a gain up to 61.11 % compared to static TIN. The gain is higher than that in Fig. 2, because in this case the dynamic clustering supports RS-CMD in interference limited regime.

B. The Role of RS-CMD

To illustrate the impact of common message decoding on performance, we plot the achievable sum rate of the common part and private part as a function of the backhaul capacity in Fig. 4. The rate of the common message increases as the backhaul capacity increases, which highlights the impact of RS-CMD as we approach the interference limited regime. Interestingly, as we increase the number of users which decode the common-messages of other users, by increasing μ we note from Fig. 5 that the rate of common messages decreases which reduces the total achievable rate.

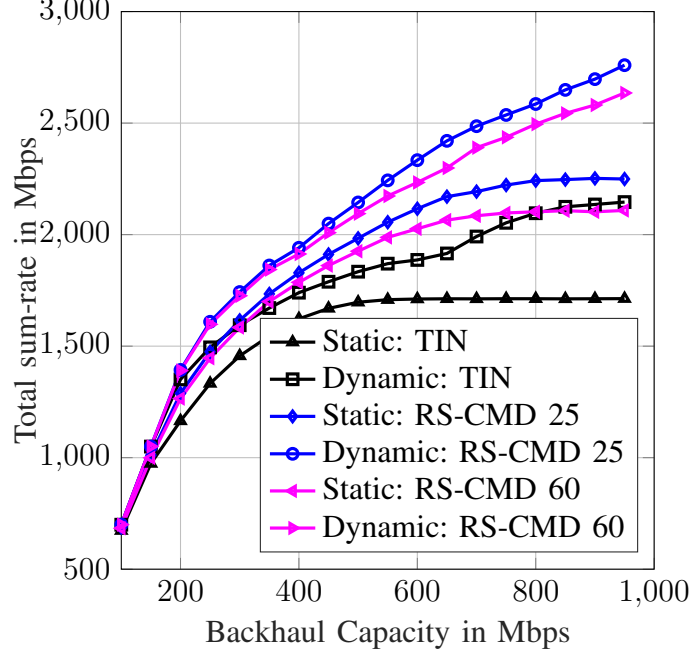


Figure 3: The performance of all studied schemes for a C-RAN with 7 BSs serving 28 users and an inter-cell distance of 400 m

C. Transmission Power Impact on RS-CMD

In this simulation set we vary the maximum transmission power per BS and we observe the achievable sum-rate. To study the impact of transmission power on the performance of RS-CMD we focus on examining the static clustering for both TIN and RS-CMD. In Fig. 6, as the transmission power increases from 0 dBm to 40 dBm we see clearly that the gain of RS-CMD compared to TIN increases. In case of $\mu = 25$ the gain of RS-CMD over TIN increases from about 12% at 0dBm maximum transmission power to almost 19% at 40dBm. Intuitively, as the transmission power increases the interference experienced in the network increases as well. Hence, the effectiveness of RS-CMD becomes more pronounced since this method is originally designed to mitigate the interference, while using TIN becomes sub-optimal in high interference regimes.

D. Convergence behavior of algorithms 2 and 3

We conduct some numerical simulations to illustrate the convergence of Algorithms 2 and 3, to a stationary solution as indicated in Theorem 1. All the simulation results are averaged over 80 random realization of the studied network of 400 m inter-cell distance. The criteria to stop

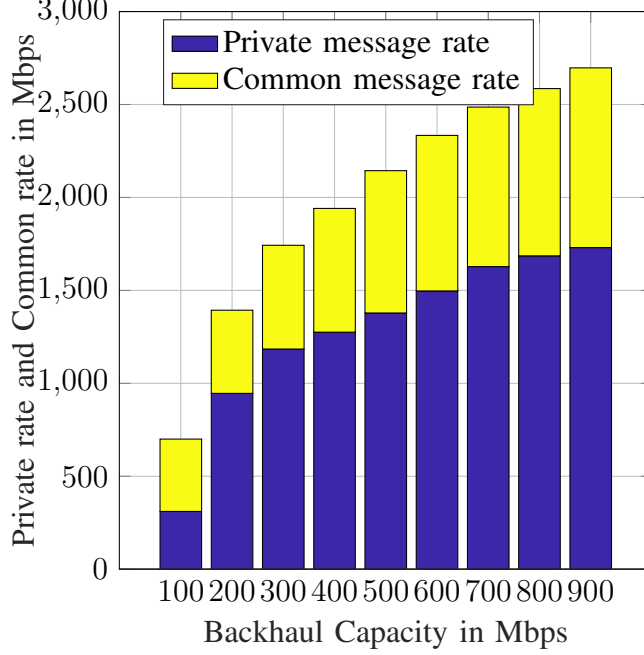


Figure 4: The sum-rate of common message and private message using RS-CMD with $\mu = 25$ for a C-RAN with 7 BSs serving 28 users and an inter-cell distance of 400 m

Algorithm 2, is when the objective improvement is less than a specific tolerance, or when the association variables $t_{n,k}$ does not change significantly after a certain iteration, indicating that the formed clusters of each user already stabilized. In fact, we have observed that the clusters converge after few iterations and therefore the algorithm terminates after a specific number of iterations, which is chosen to be 25 in these simulations since no further improvement can be achieved by continuing the process. In Fig. 7, we show the objective function of problem (39) as a function of the number of iterations. Here, Algorithm 2 is applied using RS-CMD for backhaul capacities of $C_n = 100$ Mbps, 450 Mbps and 950 Mbps. For Algorithm 3 we get the Figure 8. We clearly see from Fig. 8 that only few iterations are needed to find a stationary solution within the accuracy tolerance we choose. Interestingly, for low backhaul capacities we need much lower number of iterations to converge compared with higher backhaul capacities. The intuition behind this is that as we increase the backhaul capacity, the search space in the optimization problem becomes larger and hence it takes more effort to obtain the stationary solution.

E. The impact of the number of users on the performance

Last but not least we examine the impact of increasing the number of users at the network on the achievable performance.

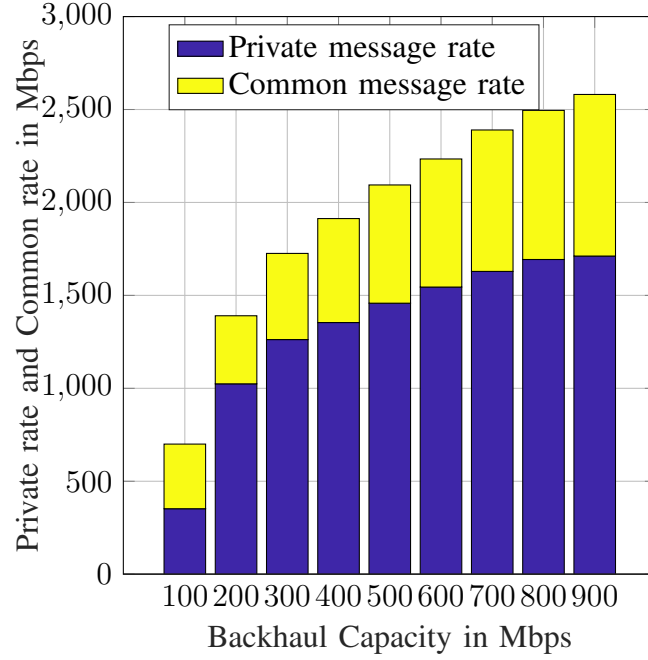


Figure 5: The sum-rate of common message and private message using RS-CMD with $\mu = 60$ for a C-RAN with 7 BSs serving 28 users and an inter-cell distance of 400 m

VI. CONCLUSIONS

This paper amalgamates the benefits of RS in C-RAN for enabling large-scale interference management. It solves the problem of maximizing the weighted sum-rate subject to finite backhaul capacity and transmission power constraints. Simulations show that the RS scheme outperforms the conventional private-information transmission approach. The gain is more significant in dense networks as well as interference limited regimes.

REFERENCES

- [1] A. A. Ahmad, H. Dahrouj, A. Chaaban, A. Sezgin, and M. Alouini, "Interference mitigation via rate-splitting in cloud radio access networks," in *2018 IEEE 19th International Workshop on Signal Processing Advances in Wireless Communications (SPAWC)*, June 2018, pp. 1–5.
- [2] J. G. Andrews, S. Buzzi, W. Choi, S. V. Hanly, A. Lozano, A. C. K. Soong, and J. C. Zhang, "What will 5g be?" *IEEE Journal on Selected Areas in Communications*, vol. 32, no. 6, pp. 1065–1082, June 2014.
- [3] L. B. Le, V. Lau, E. Jorswieck, N.-D. Dao, A. Haghighat, D. I. Kim, and T. Le-Ngoc, "Enabling 5g mobile wireless technologies," *EURASIP Journal on Wireless Communications and Networking*, vol. 2015, no. 1, p. 218, Sep 2015. [Online]. Available: <https://doi.org/10.1186/s13638-015-0452-9>

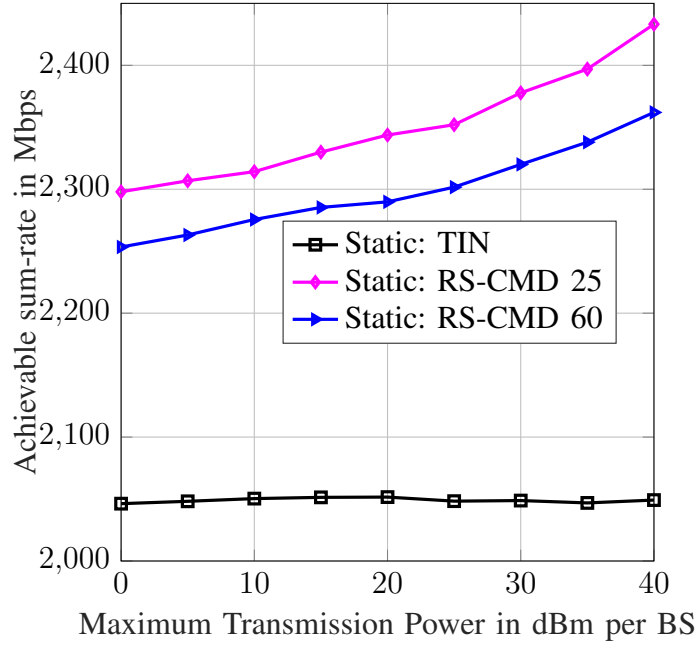


Figure 6: The achievable sum-rate as a function of maximum transmission power, using static TIN and RS-CMD with $\mu = 25$ for the scenario in which a C-RAN with 7 BSs serving 28 users. Each BS has 750 Mbps backhaul. The inter-cell distance is 200 m

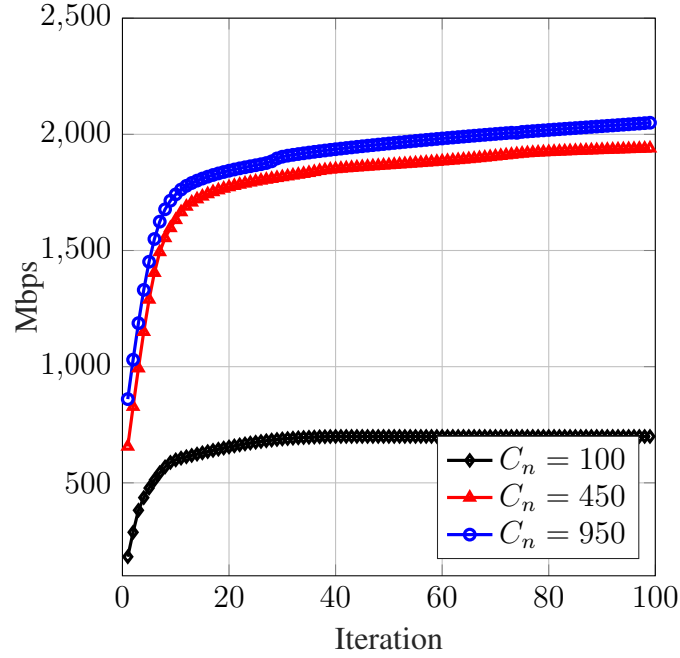


Figure 7: The objective function of (39), using RS-CMD with $\mu = 25$ for the scenario in which a C-RAN with 7 BSs serving 28 users and an inter-cell distance of 400 m

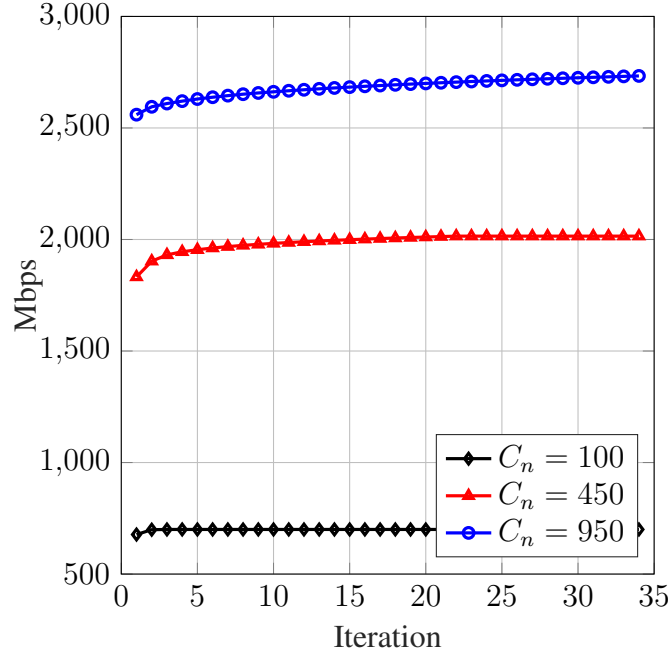


Figure 8: The objective function of (39), using RS-CMD with $\mu = 25$ for the scenario in which a C-RAN with 7 BSs serving 28 users and an inter-cell distance of 400 m

- [4] N. Bhushan, J. Li, D. Malladi, R. Gilmore, D. Brenner, A. Damnjanovic, R. T. Sukhavasi, C. Patel, and S. Geirhofer, "Network densification: the dominant theme for wireless evolution into 5g," *IEEE Communications Magazine*, vol. 52, no. 2, pp. 82–89, February 2014.
- [5] D. Wubben, P. Rost, J. S. Bartelt, M. Lalam, V. Savin, M. Gorgoglione, A. Dekorsy, and G. Fettweis, "Benefits and impact of cloud computing on 5g signal processing: Flexible centralization through cloud-RAN," *IEEE Signal Processing Magazine*, vol. 31, no. 6, pp. 35–44, Nov 2014.
- [6] O. Simeone, A. Maeder, M. Peng, O. Sahin, and W. Yu, "Cloud radio access network: Virtualizing wireless access for dense heterogeneous systems," *Journal of Communications and Networks*, vol. 18, no. 2, pp. 135–149, April 2016.
- [7] Y. Shi, J. Zhang, and K. B. Letaief, "Group sparse beamforming for green cloud-ran," *IEEE Transactions on Wireless Communications*, vol. 13, no. 5, pp. 2809–2823, May 2014.
- [8] M. Peng, C. Wang, V. Lau, and H. V. Poor, "Fronthaul-constrained cloud radio access networks: insights and challenges," *IEEE Wireless Communications*, vol. 22, no. 2, pp. 152–160, April 2015.
- [9] J. Tang, W. P. Tay, and T. Q. S. Quek, "Cross-layer resource allocation with elastic service scaling in cloud radio access network," *IEEE Transactions on Wireless Communications*, vol. 14, no. 9, pp. 5068–5081, Sep. 2015.
- [10] M. Tao, E. Chen, H. Zhou, and W. Yu, "Content-centric sparse multicast beamforming for cache-enabled cloud RAN," *IEEE Transactions on Wireless Communications*, vol. 15, no. 9, pp. 6118–6131, Sep. 2016.
- [11] Y. Ugur, Z. H. Awan, and A. Sezgin, "Cloud radio access networks with coded caching," *WSA 2016; 20th International ITG Workshop on Smart Antennas*, pp. 1–5, March 2016.
- [12] A. Alameer and A. Sezgin, "Joint beamforming and network topology optimization of green cloud radio access networks," in *2016 9th International Symposium on Turbo Codes and Iterative Information Processing (ISTC)*, Sep. 2016, pp. 375–379.
- [13] A. Alameer and A. Sezgin, "Resource cost balancing with caching in C-RAN," *2017 IEEE Wireless Communications and Networking Conference (WCNC)*, pp. 1–6, March 2017.

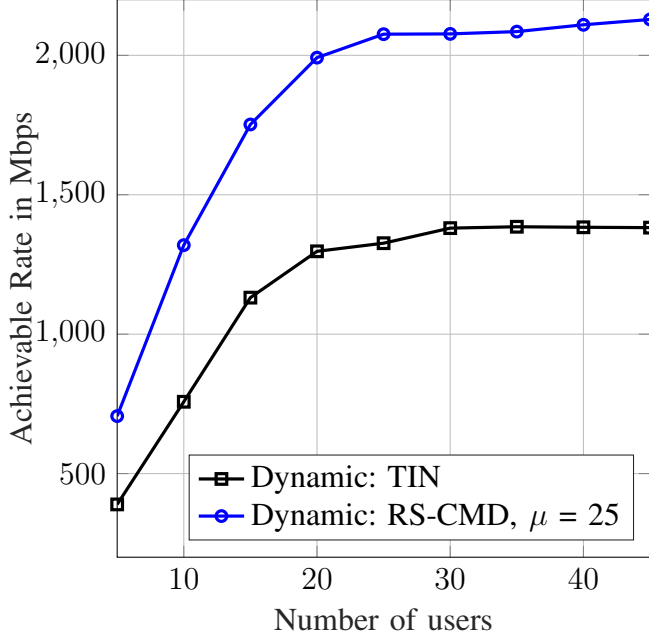


Figure 9: The achievable sum-rate, using dynamic RS-CMD with $\mu = 25$ and dynamic TIN for the scenario in which a C-RAN with 7 BSs serving 28 users. Each BS has 4 Antenna. The inter-cell distance is 200 m

- [14] T. Han and K. Kobayashi, "A new achievable rate region for the interference channel," *IEEE Transactions on Information Theory*, vol. 27, no. 1, pp. 49–60, January 1981.
- [15] R. H. Etkin, D. N. C. Tse, and H. Wang, "Gaussian interference channel capacity to within one bit," *IEEE Transactions on Information Theory*, vol. 54, no. 12, pp. 5534–5562, Dec 2008.
- [16] O. Simeone, O. Somekh, H. V. Poor, and S. Shamai (Shitz), "Downlink multicell processing with limited-backhaul capacity," *EURASIP Journal on Advances in Signal Processing*, vol. 2009, no. 1, p. 840814, Jun 2009.
- [17] S. Park, O. Simeone, O. Sahin, and S. Shamai, "Joint precoding and multivariate backhaul compression for the downlink of cloud radio access networks," *IEEE Transactions on Signal Processing*, vol. 61, no. 22, pp. 5646–5658, Nov 2013.
- [18] R. Zakhour and D. Gesbert, "Optimized data sharing in multicell mimo with finite backhaul capacity," *IEEE Transactions on Signal Processing*, vol. 59, no. 12, pp. 6102–6111, Dec 2011.
- [19] B. Dai and W. Yu, "Sparse beamforming and user-centric clustering for downlink cloud radio access network," *IEEE Access*, vol. 2, pp. 1326–1339, 2014.
- [20] L. Liu and W. Yu, "Cross-layer design for downlink multihop cloud radio access networks with network coding," *IEEE Transactions on Signal Processing*, vol. 65, no. 7, pp. 1728–1740, April 2017.
- [21] H. Dahrouj and W. Yu, "Multicell interference mitigation with joint beamforming and common message decoding," *IEEE Transactions on Communications*, vol. 59, no. 8, pp. 2264–2273, August 2011.

- [22] O. Sahin, J. Li, Y. Li, and P. J. Pietraski, "Interference mitigation via successive cancellation in heterogeneous networks," in *2011 8th International Symposium on Wireless Communication Systems*, Nov 2011, pp. 720–724.
- [23] E. Che, H. D. Tuan, H. H. M. Tam, and H. H. Nguyen, "Successive interference mitigation in multiuser MIMO channels," *IEEE Transactions on Communications*, vol. 63, no. 6, pp. 2185–2199, June 2015.
- [24] Y. Mao, B. Clerckx, and V. O. K. Li, "Rate-splitting for downlink multi-user multi-antenna systems: Bridging NOMA and conventional linear precoding," *EURASIP Journal on Wireless Communications and Networking*, 2018.
- [25] Y. Mao and B. Clerckx and V. O. K. Li, "Energy efficiency of rate-splitting multiple access, and performance benefits over sdma and noma," in *2018 15th International Symposium on Wireless Communication Systems (ISWCS)*, Aug 2018, pp. 1–5.
- [26] Y. Mao, B. Clerckx, and V. O. K. Li, "Rate-splitting for multi-antenna non-orthogonal unicast and multicast transmission," in *2018 IEEE 19th International Workshop on Signal Processing Advances in Wireless Communications (SPAWC)*, June 2018, pp. 1–5.
- [27] E. Karipidis, N. D. Sidiropoulos, and Z. Luo, "Quality of service and max-min fair transmit beamforming to multiple cochannel multicast groups," *IEEE Transactions on Signal Processing*, vol. 56, no. 3, pp. 1268–1279, March 2008.
- [28] H. Dahrouj and W. Yu, "Coordinated beamforming for the multicell multi-antenna wireless system," *IEEE Transactions on Wireless Communications*, vol. 9, no. 5, pp. 1748–1759, May 2010.
- [29] D. Gesbert, S. Hanly, H. Huang, S. S. Shitz, O. Simeone, and W. Yu, "Multi-cell MIMO cooperative networks: A new look at interference," *IEEE Journal on Selected Areas in Communications*, vol. 28, no. 9, pp. 1380–1408, December 2010.
- [30] W. Yu, T. Kwon, and C. Shin, "Multicell coordination via joint scheduling, beamforming and power spectrum adaptation," in *2011 Proceedings IEEE INFOCOM*, April 2011, pp. 2570–2578.
- [31] D. W. H. Cai, T. Q. S. Quek, and C. W. Tan, "Coordinated max-min SIR optimization in multicell downlink - duality and algorithm," in *2011 IEEE International Conference on Communications (ICC)*, June 2011, pp. 1–6.
- [32] Y. Huang, C. W. Tan, and B. D. Rao, "Joint beamforming and power control in coordinated multicell: Max-min duality, effective network and large system transition," *IEEE Transactions on Wireless Communications*, vol. 12, no. 6, pp. 2730–2742, June 2013.
- [33] N. Naderializadeh and A. S. Avestimehr, "ITLinQ: A new approach for spectrum sharing in device-to-device communication systems," *IEEE Journal on Selected Areas in Communications*, vol. 32, no. 6, pp. 1139–1151, June 2014.
- [34] X. Wu, S. Tavildar, S. Shakkottai, T. Richardson, J. Li, R. Laroia, and A. Jovicic, "FlashLinQ: A synchronous distributed scheduler for peer-to-peer ad hoc networks," *IEEE/ACM Transactions on Networking*, vol. 21, no. 4, pp. 1215–1228, Aug 2013.
- [35] X. Yi and G. Caire, "Optimality of treating interference as noise: A combinatorial perspective," *IEEE Transactions on Information Theory*, vol. 62, no. 8, pp. 4654–4673, Aug 2016.
- [36] E. Chen and M. Tao, "Backhaul-constrained joint beamforming for non-orthogonal multicast and unicast transmission," in *GLOBECOM 2017 - 2017 IEEE Global Communications Conference*, Dec 2017, pp. 1–6.
- [37] A. A. Nasir and H. D. Tuan and T. Q. Duong and H. V. Poor, "Secure and energy-efficient beamforming for simultaneous information and energy transfer," *IEEE Transactions on Wireless Communications*, vol. 16, no. 11, pp. 7523–7537, Nov 2017.
- [38] S. Boyd and L. Vandenberghe, *Convex Optimization*. Cambridge University Press, 2004.
- [39] G. Scutari, F. Facchinei, and L. Lampariello, "Parallel and distributed methods for constrained nonconvex optimization—part I: Theory," *IEEE Transactions on Signal Processing*, vol. 65, no. 8, pp. 1929–1944, April 2017.
- [40] M. S. Lobo, L. Vandenberghe, S. Boyd, and H. Lebret, "Applications of second-order cone programming," *Linear Algebra and its Applications*, vol. 284, no. 1, pp. 193 – 228, 1998, international Linear Algebra

Society (ILAS) Symposium on Fast Algorithms for Control, Signals and Image Processing. [Online]. Available: <http://www.sciencedirect.com/science/article/pii/S0024379598100320>